Boletim da Sociedade Astronômica Brasileira, **35**, no. 1, 3-6

A tricky inverse problem:

The information content of galaxy spectra

Ignacio Ferreras[1,2,3]

[1] Instituto de Astrofísica de Canarias, Calle Vía Láctea s/n, E-38205, La Laguna, Tenerife, Spain
[2] Department of Physics and Astronomy, University College London, London WC1E 6BT, UK
[3] Departamento de Astrofísica, Universidad de La Laguna, E-38206 La Laguna, Tenerife, Spain
e-mail: i.ferreras@ucl.ac.uk

Abstract. Galaxy spectra encode valuable information concerning the visible constituents: stellar populations, gas and dust. We focus on the former, asking a basic question: "What is the maximum amount of information that can be extracted from the stars?". While stellar populations, in principle, could give most of the details about the way a galaxy is formed, the inherent limitations caused by the entanglement of this information in the spectra reduces the output to a few parameters, most notably average age, chemical composition, and a general abundance ratio between key elements. In this keynote talk I will present the problem from a fundamental point of view based on information theory.

Resumo. O espectro de uma galáxia contém informações valiosas sobre o que a compõem: população estelar, gás e poeira. Nós focamos no primeiro, tentando responder uma questão fundamental: "Qual é o máximo de informação que pode ser extraído da componente estelar em um espectro?". Embora as populações estelares, em princípio, possam fornecer a maioria dos detalhes sobre a formação de uma galáxia, as limitações inerentes causadas pelo emaranhamento dessas informações nos espectros reduzem o número de parâmetros realmente independentes. Em geral, acaba por limitar a inferência a comparações de idade média, composição química e razão entre a abundância de alguns elementos chave. Nesta palestra plenária, eu vou analisar este paradigma utilizando como base o ponto de vista fundamental da teoria da informação.

Keywords. Galaxies: evolution – Galaxies: stellar content – Techniques: spectroscopic – Methods: statistical

1. Introduction

Of the various components that galaxies are made of, stars arguably produce the majority of the observables that allow us to backtrack their formation histories. While gas is undoubtedly a strong contender (in its different phases), the light emitted from this component is mostly restricted to relatively short timescales. Due to the longer stellar lifetimes (especially lower mass stars) and collisionless nature, the stellar populations encode the transformation of gas into stars along with relevant dynamical events for many Gyr. Therefore, one of the major goals in extragalactic astrophysics is how to extract this information from the best possible observable: spectra. Figure 1 illustrates this problem by showing the star formation history of a synthetic galaxy from the Illustris TNG-100 simulation (Nelson et al. 2019, *left*), and the resulting galaxy spectrum (*right*). The spectrum is a superposition of all the different stars over their corresponding intervals of age, metallicity and mass (here produced from the population synthesis models of Vazdekis et al. 2012). If we marginalise the 2D distribution over the metallicity (horizontal) axis, we produce the so-called star formation history (SFH), that mainly depends on the various events that lead to gas flows that trigger star formation, such as the cooling and collapse of the gas in a halo towards the central region, merging processes, or secular events that rearrange the orbits allowing for gas inflows. If we marginalise over the age (vertical) axis, we produce the chemical enrichment history (CEH) that is more relevant to the details of the gas flows (infall vs outflows, mergers of low-mass systems, etc). The holy grail in this process would be to invert this problem, so that from an observed spectrum one could recover the 2D distribution shown on the left panel of Figure 1. Alas, this inverse problem is plagued with numerous degeneracies caused by the superposition of stellar atmospheres whose spectra look similar and could correspond to very different properties. Moreover, the motion of the stars produce a spectral smoothing that limits the effective resolution to, at best, $R \equiv \lambda/\Delta\lambda \lesssim 5000$. This contribution focuses on a critical view of how observations can produce detailed information about the underlying formation histories of galaxies. Since we focus on the stellar content, I will restrict the analysis to the NUV-optical-NIR spectral window, as most of the photons from stellar atmospheres are produced in this interval. I will therefore omit other contributors such as diffuse gas, dust, etc, that would only complicate things further.

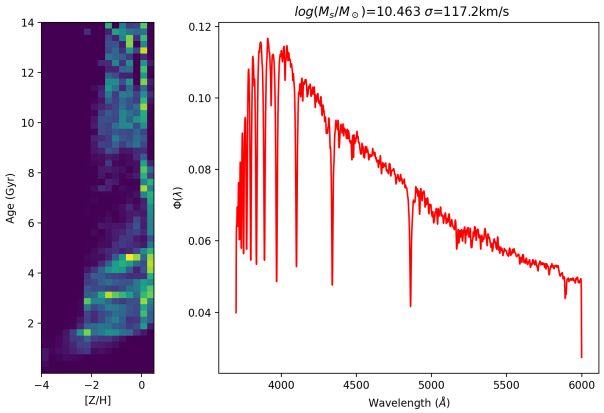

Figura 1. Illustration of the main goal: extracting SFHs and CEHs from spectra.

Para cópias, contate: I. Ferreras

The traditional approach, since the very first steps on stellar population synthesis (e.g. Tinsley 1980) was based on a model comparison between an observable (photometric or spectroscopic) and a model that depends on a reduced set of free parameters – mainly age, stellar initial mass function and chemical composition – to describe a stellar population. Simple stellar populations (SSPs) are built at a fixed set of those parameters, and linear superposition of SSP-derived observables are compared to the real data to constrain those free parameters. At the simplest level, one can fit the populations in a globular cluster or a massive elliptical galaxy, systems where an SSP approximation is justified (to some degree, see, for instance, the contribution of Corinne Charbonnel to this meeting). More general cases invoke pre-defined sets of SFHs and CEHs (either from generic functions or simulations-based data). Standard statistical methods define a goodness of fit, including a Bayesian approach that allows for the derivation of the corresponding uncertainties. There has been a large industry on constraining stellar population properties this way (excellent reviews can be found in Walcher et al. 2011 and Conroy 2013) with methods that include full spectral fitting (e.g. Cid Fernandes et al. 2005; Cappellari 2023), or the analysis of a reduced, well-defined set of absorption features (e.g. Trager et al. 1998; Rogers et al. 2010). As usual with any model fitting, one should be aware of the potential systematics induced by the models themselves – or by some property inherent to the method. As an illustration, Figure 2 shows the time gradient (with respect to the logarithm of stellar age, much more appropriate in this case) of three observables: $(u-g)$ colour (in the SDSS system), the 4000Å break strength defined by Balogh et al. (1999), and a Balmer absorption index, Hδ_F (Worthey & Ottaviani 1997). The synthesis models of Vazdekis et al. (2012) have been used here at solar metallicity, but other models produce very similar results. Note the strong age dependence of the Hδ_F index, often used to characterize stellar populations. However, not only is this index very sensitive to age, but its variation is strongest over a relatively narrow interval of stellar age, around 0.4–1 Gyr, which is expected from the fact that the presence of Balmer absorption is strongest in the stellar atmospheres of A-type stars. Unsurprisingly, the Main Sequence turnoff time for this type of star happens to be in that age range. While this result is intrinsic to the properties of stellar populations, we should be aware of this potential systematic: adopting an index that is mostly sensitive to ∼1 Gyr ages may end up biasing any estimate to this timescale. There are other shortcomings of synthetic population models, such as the use of empirical libraries that are inescapably restricted to the solar neighbourhood (e.g., Sánchez-Blázquez et al. 2006), or rely on theoretical atmosphere models, with the associated problems in the modelling of absorption lines (e.g. Coelho 2014). A number of computer codes have become available to the aficionados so that they can constrain the stellar populations in a rather user-friendly way (see Pacifici et al. 2023, for a comparison of some of these methods). The focus of this contribution is not about these methods or even about synthesis models, but aims at a more fundamental question: "How accurately can we derive a SFH/CEH from galaxy spectra?"

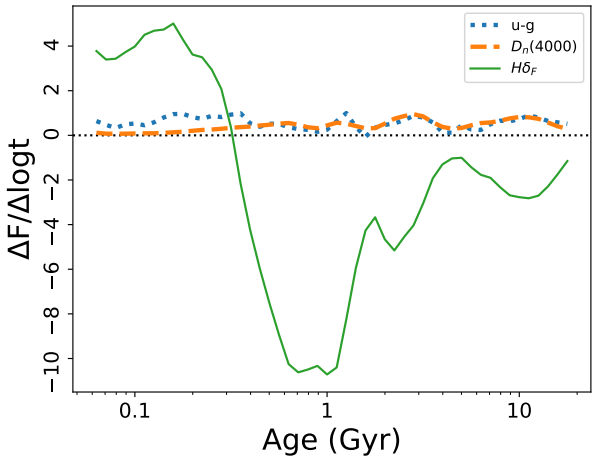

Figura 2. Time derivatives of typical observables used in the analysis of stellar ages ($F = \{(u-g), D_n(4000), H\delta_F\}$, as labelled). The synthetic models are from Vazdekis et al. (2012).

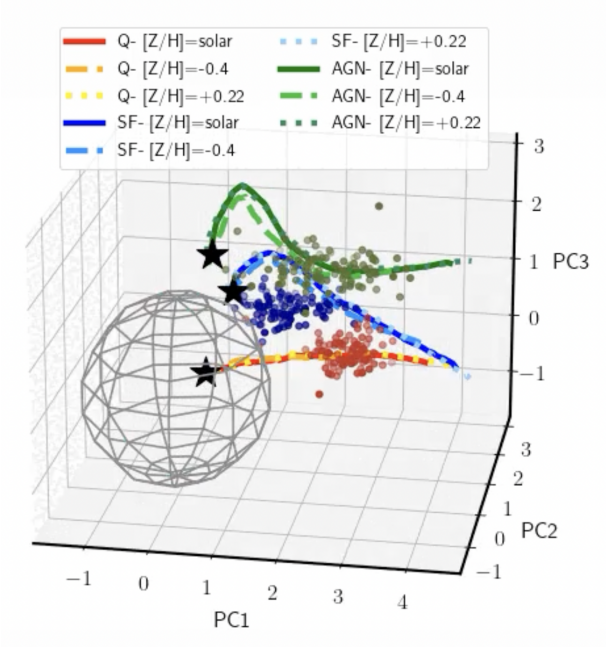

Figura 3. Projection in 3D latent space (PCA) of a sample of SDSS galaxy spectra segregated with respect to nebular activity into quiescent (Q), star-forming (SF) and AGN. The lines correspond to predictions from the MIUSCAT models (Vazdekis et al. 2012). Adapted from an animated figure presented in Sharbaf et al. (2023).

2. A multivariate approach

In its most basic form, the analysis of galaxy spectra constitutes a multivariate problem, where the observation of a set of M galaxies, given by $\mathbf{y}_{i,j} \equiv \Phi_j(\lambda_i)$, i.e. evaluated at N spectral intervals, can be written in terms of a set of M "base spectra", $\{\mathbf{x}_{i,j}\}$ $(i = 1,\ldots,N;\ j = 1,\ldots,M)$, via some mixing matrix $\mathcal{W}$:

$$\boldsymbol{y} = \mathcal{W}\boldsymbol{x}(+\epsilon) \Longrightarrow \boldsymbol{x} = \mathcal{W}^{-1}(\boldsymbol{y} - \epsilon), \qquad (1)$$

where ϵ represents a noise term that we assume fully understood. Even in this most ideal assumption, the derivation of the base spectra and the mixing matrix is an unsurmountable challenge. The traditional method would make use of synthetic populations as the base spectra, but could it be possible to have a data-driven derivation of the base spectra from a large sample of observations, in a model-independent way (thus free from the inherent systematics)?

Applications of this methodology can be found in the literature, making use of multivariate algorithms such as Principal Component Analysis (PCA, e.g., Rogers et al. 2007), Factor Analysis (FA, e.g., Nolan, Raychaudhury, & Kabán 2007) or independent component analysis (ICA, e.g., Lu et al. 2006). While some interesting results were found, the upshot is that the spectra could only be separated with respect to average stellar age,

a well-known result since younger populations are dominated by massive, blue and luminous stars, whereas older populations feature only low mass, red, fainter stars. This is, for instance, the cause of the galaxy bimodality found on a colour-mass plot, that defines a so-called red sequence dominated by quiescent galaxies and a blue cloud formed by star-forming systems (e.g. Angthopo et al. 2019). Even at the "next level", concerning chemical composition, these data-driven methods are not capable of discerning the age-metallicity degeneracy (Worthey 1994) where the effects of stellar age or chemical composition are very similar, even with targeted line strengths, that, in principle, are more sensitive to either age or metallicity. Figure 3 (adapted from Sharbaf et al. 2023) nicely illustrates the strong, intrinsic, degeneracy on a latent space formed by projections on the three eigenvectors with the highest variance, applying PCA to a set of spectra from the Sloan Digital Sky Survey (SDSS). The sample is split according to nebular emission into quiescent (Q), star-forming (SF) and AGN, although the analysis is performed on continuum-subtracted data with emission lines removed from the analysis. Each subset is shown as coloured data points, and the predictions simple stellar populations are given by lines (corresponding to a range of age, with the star symbol corresponding to the youngest SSP). Three choices of metallicity are considered, at solar, sub-solar and super-solar chemical composition, as labelled. Note that in this 3D latent space, purely determined by the three highest components in variance of the data, the tracks for different metallicities just slide along one another, i.e. a population with a given age and metallicity can be simply mapped for another metallicity by choosing a different age, but no other substantial variations are found at this level of detail. We emphasize here that the traditional methods based on targeted line strengths can mitigate this degeneracy to some degree, but the result presented in Figure 3 illustrates the fundamental challenge in overcoming this degeneracy.

3. The information content: entropy

So far we have considered two alternative interpretations of galaxy spectra: 1) A wavelength-dependent function that is compared with models whose parameters are fit with some statistic; and 2) a multi-dimensional vector, so that samples of spectra can be explored using multivariate methods such as principal component analysis. A third option is to interpret a spectrum as a probability distribution, a concept inspired by photon counting detectors. In this case, the associated probability distribution: $\Phi(\lambda) \longrightarrow \mathcal{P}(\lambda)$ allows us to define entropy, as in information theory: $\mathcal{H} \equiv -\int \mathcal{P}(\lambda) \log \mathcal{P}(\lambda)$. However, a practical implementation restricts the integral within some interval $\Delta\lambda$ centred at some wavelength λ, so that we can define a so-called entropy spectrum, $\mathcal{H}_{\Delta\lambda}(\lambda)$. The interval $\Delta\lambda$ is optimally chosen to be narrow enough to trace the variations in the spectra but not too narrow to avoid being overly sensitive to noise or the velocity dispersion of the spectra. In typical galaxy spectra with resolution $\mathcal{R} \sim$2,000 a valid choice is $\Delta\lambda = 100$Å. Figure 4 compares the negentropy[1] spectrum of three choices of synthetic models from Bruzual & Charlot (2003, left panel) with a sample of galaxies from SDSS (see Ferreras et al. 2023, for full details of this analysis). Similarly to the data in Figure 3, the observed sample is split into quiescent, star-forming or AGN, based on the emission lines of the diffuse gas. We discard emission lines in the analysis, except for this classification, as we are focusing on the stellar population themselves, i.e. on the photons originating in stellar atmospheres. The most remarkable result is that the information – measured as negentropy – is located in a rather small set of wavelength intervals, the most prominent shown as shaded orange regions. Any code based on data-driven analysis – including the most sophisticated Deep Learning algorithms (see, e.g., Lovell et al. 2019; Portillo et al. 2020; Melchior et al. 2023) – will make use of this information to learn from the spectra. It comes as no surprise that the six regions marked in the figure are those most often used in analyses of the stellar population content of galaxies. This result confirms the previous result from §2 in the sense that only a reduced set of "latent variables" can be meaningfully extracted from galaxy spectra, reducing the ability to constrain detailed SFHs or CEHs. Also note that the actual values of negentropy in Figure 4 are rather small, $O(10^{-3})$, which confirms the effectively low information content (a fully random probability distribution would give $\bar{\mathcal{H}} = 0$).

[1] Negentropy ($\bar{\mathcal{H}}_{\Delta\lambda}$) is defined as the complement of entropy ($1 - \mathcal{H}_{\Delta\lambda}$), so that maximal entropy (by definition, $\mathcal{H}_{\Delta\lambda} = 1$) means minimal information, or negentropy ($\bar{\mathcal{H}}_{\Delta\lambda} = 0$)

4. Conclusions

This contribution focuses on the amount of information that can be learned from galaxy spectra, following a fundamental approach based on the sheer ability of extracting variations from the data. Galaxy spectra are highly correlated structures, something that effectively reduces the true dimensionality of the input data. This explains, for instance, why a handful of line strengths have the same constraining power as thousands of spectral data $\{\Phi(\lambda_i)\}$, as the covariance of those is very high. The question remains whether one can define an algorithm that could determine SFHs and CEHs from observational data – if only in a statistical way – beyond the lowest order estimates such as average age, metallicity, or [Mg/Fe]. Such a method needs to confront the high level of entanglement of the input data, and traditional model fitting data seem not to be good enough for this most challenging task. To illustrate how important it is to define a proper algorithm to solve this problem, Figure 5 shows the scree plot – the decreasing variance with respect to rank for a PCA decomposition – corresponding to three types of input for the same set of synthetic galaxies retrieved from the Illustris-TNG100 simulations (Nelson et al. 2019). The blue dotted line shows the result when using the actual star formation histories: this corresponds to the ideal case, where the full information is available. The red dashed line perfoms PCA on the resulting spectra for each galaxy, i.e. combining the SFH with population synthesis models (the 3700-6000Å spectral rest-frame window is adopted, at $\mathcal{R}$=2,000). Note the dramatic difference between these two scree plots: the spectral data (a projection on to an "observable plane") are significantly more compressible (steeper scree plot), a sign of the substantial drop in information due to the projection. Interestingly, PCA on the six values of the entropy spectra defined by the orange regions shown in Figure 4 (excluding Hα to avoid emission line contamination) suggests that the information loss can be mitigated.

Agradecimentos. Gostaria de agradecer calorosamente aos organizadores do SAB 2023 pelo gentil convite e por tão grande encontro. I acknowledge support from the Spanish Research Agency of the Ministry of Science and Innovation (AEI-MICINN) under the grant with reference PID2019-104788GB-I00.

Referências

Angthopo J., Ferreras I., Silk J., 2019, MNRAS, 488, L99
Balogh M. L., Morris S. L., Yee H. K. C., Carlberg R. G., Ellingson E., 1999, ApJ, 527, 54
Bruzual G., Charlot S., 2003, MNRAS, 344, 1000
Cappellari M., 2023, MNRAS, 526, 3273

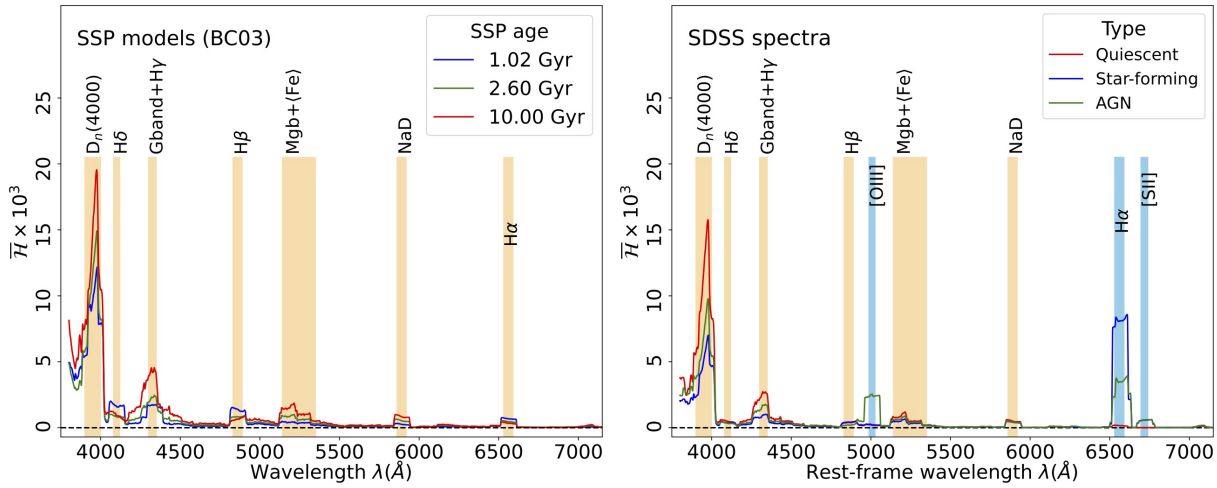

Figura 4. *Left:* Negentropy spectrum of three Simple Stellar Populations from the synthesis models of Bruzual & Charlot (2003), at solar composition, with ages as labelled. *Right:* Equivalent case for a set of SDSS galaxy spectra split into quiescent, star-forming, and AGN.

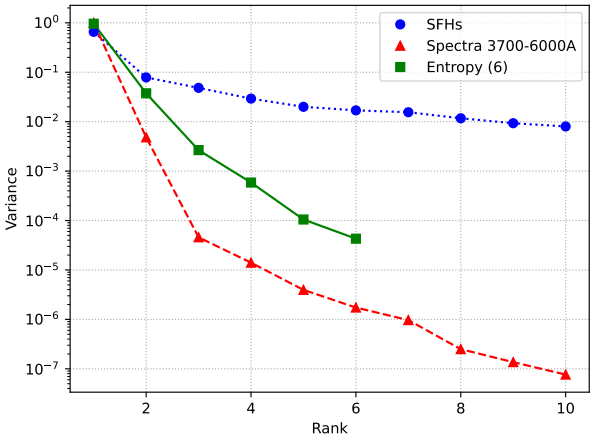

Figura 5. Scree plot (variance drop in a PCA decomposition) for three types of input data from synthetic galaxies extracted from the Illustris-TNG100 simulations (Nelson et al. 2019).

Cid Fernandes R., Mateus A., Sodré L., Stasińska G., Gomes J. M., 2005, MNRAS, 358, 363
Coelho P. R. T., 2014, MNRAS, 440, 1027
Conroy C., 2013, ARA&A, 51, 393
Ferreras, I., Lahav, O., Somerville, R. S., Silk, J., 2023, RASTI, 2, 78
Lovell C. C., Acquaviva V., Thomas P. A., Iyer K. G., Gawiser E., Wilkins S. M., 2019, MNRAS, 490, 5503
Lu H., Zhou H., Wang J., Wang T., Dong X., Zhuang Z., Li C., 2006, AJ, 131, 790
Melchior P., Liang Y., Hahn C., Goulding A., 2023, AJ, 166, 74
Nelson D., Springel V., Pillepich A., Rodriguez-Gomez V., Torrey P., Genel S., Vogelsberger M., et al., 2019, ComAC, 6, 2
Nolan L. A., Raychaudhury S., Kabán A., 2007, MNRAS, 375, 381
Pacifici C., Iyer K. G., Mobasher B., da Cunha E., Acquaviva V., Burgarella D., Calistro Rivera G., et al., 2023, ApJ, 944, 141
Portillo S. K. N., Parejko J. K., Vergara J. R., Connolly A. J., 2020, AJ, 160, 45
Rogers B., Ferreras I., Lahav O., Bernardi M., Kaviraj S., Yi S. K., 2007, MNRAS, 382, 750
Rogers B., Ferreras I., Peletier R., Silk J., 2010, MNRAS, 402, 447
Sánchez-Blázquez P., Peletier R. F., Jiménez-Vicente J., Cardiel N., Cenarro A. J., Falcón-Barroso J., Gorgas J., et al., 2006, MNRAS, 371, 703
Sharbaf Z., Ferreras I., Lahav O., 2023, MNRAS, 526, 585
Tinsley B. M., 1980, FCPh, 5, 287
Trager S. C., Worthey G., Faber S. M., Burstein D., González J. J., 1998, ApJS, 116, 1
Vazdekis A., Ricciardelli E., Cenarro A. J., Rivero-González J. G., Díaz-García L. A., Falcón-Barroso J., 2012, MNRAS, 424, 157
Walcher J., Groves B., Budavári T., Dale D., 2011, Ap&SS, 331, 1
Worthey G., 1994, ApJS, 95, 107
Worthey G., Ottaviani D. L., 1997, ApJS, 111, 377